Kinetics of the hydrogen abstraction $\cdot C_2H_5$ + alkane → C_2H_6 + alkyl reaction class: an application of the reaction class transition state theory

Artur Ratkiewicz, Lam K. Huynh, Quoc B. Pham & Thanh N. Truong

Theoretical Chemistry Accounts
Theory, Computation, and Modeling

ISSN 1432-881X
Volume 132
Number 3

Theor Chem Acc (2013) 132:1-17
DOI 10.1007/s00214-013-1344-x

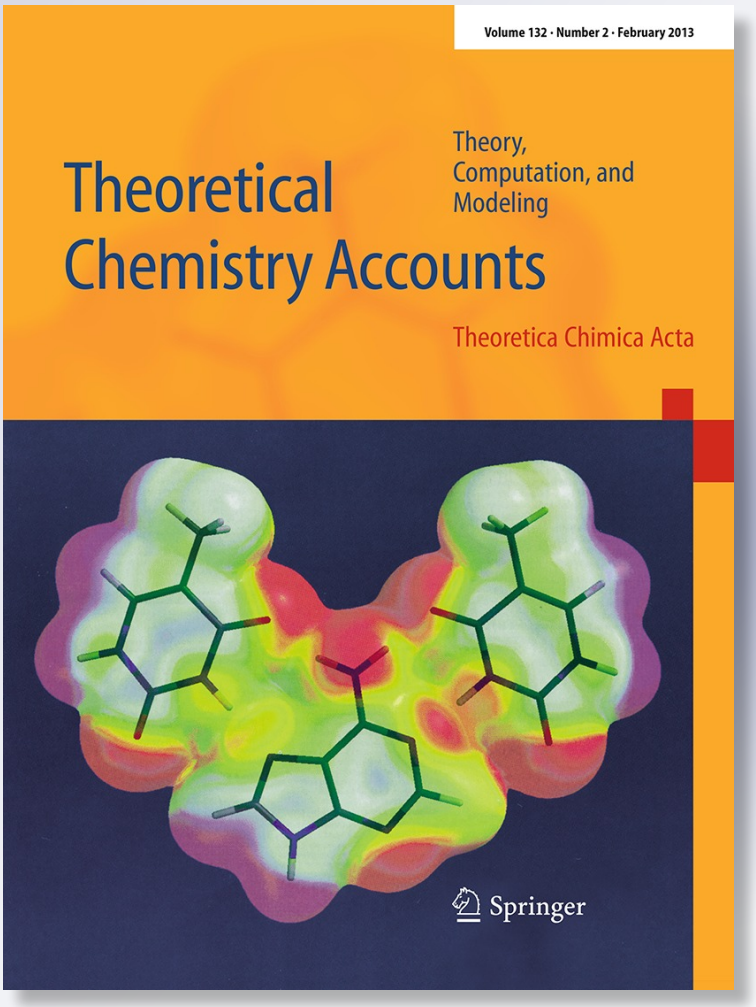

Springer

Theor Chem Acc (2013) 132:1344
DOI 10.1007/s00214-013-1344-x

REGULAR ARTICLE

Kinetics of the hydrogen abstraction $\cdot C_2H_5$ + alkane → C_2H_6 + alkyl reaction class: an application of the reaction class transition state theory

Artur Ratkiewicz · Lam K. Huynh · Quoc B. Pham · Thanh N. Truong

Received: 13 November 2012 / Accepted: 18 January 2013

Abstract This paper presents an application of the reaction class transition state theory (RC-TST) to predict thermal rate constants for hydrogen abstraction reactions at alkane by the $\cdot C_2H_5$ radical on-the-fly. The linear energy relationship (LER), developed for acyclic alkanes, was also proven to hold for cyclic alkanes. We have derived all RC-TST parameters from rate constants of 19 representative reactions, coupling with LER and the barrier height grouping (BHG) approach. Both the RC-TST/LER, where only reaction energy is needed, and the RC-TST/BHG, where no other information is needed, can predict rate constants for any reaction in this reaction class with satisfactory accuracy for combustion modeling. Our analysis indicates that less than 50 % systematic errors on the average exist in the predicted rate constants using either the RC-TST/LER or RC-TST/BHG method, while in comparison with explicit rate calculations, the differences are within a factor of 2 on the average. The results also show that the RC-TST method is not sensitive to the choice of density functional theory used.

Keywords H abstraction · Thermal rate constants · Ethyl · Combustion · Reaction class transition state theory

1 Introduction

Reactions involving hydrogen transfer between hydrocarbon fragments, like $\cdot CH_3 + RH \rightarrow \cdot CH_4 + \cdot R$ or $\cdot C_2H_5 + RH \rightarrow \cdot C_2H_6 + \cdot R$ (where ·R denotes an alkyl radical), play a significant role in the combustion of hydrocarbons [1–5]. For example, previous perfectly stirred reactor (PSR) simulations [6] of the combustion of the hydrocarbons up to n-butane performed with the Lawrence Livermore National Laboratory (LLNL) mechanism [7] show that reactions belonging to the title reaction class are sensitive to the net production of C_2H_6. Furthermore, it is also shown that the net production rates of the propyl and butyl radicals are sensitive to the rate constants of the $\cdot C_2H_5 + RH \rightarrow \cdot C_2H_6 + \cdot R$ reactions (e.g., more than 20 % change if the abstraction reactions by $\cdot C_2H_5$ are removed from the mechanisms). Alkyl products of the processes investigated in this study are key intermediates arising from the decomposition of higher hydrocarbons in essentially all flames that plays an important role in molecular weight growth chemistry leading to the production of the first aromatic rings, polycyclic aromatic hydrocarbons, and eventually soot [2]. At high temperature, long alkyls degrade rapidly into smaller fragments (normally through β-scission), which can be the primary chain carriers in thermal decomposition of hydrocarbons.

Electronic supplementary material The online version of this article (doi:10.1007/s00214-013-1344-x) contains supplementary material, which is available to authorized users.

A. Ratkiewicz (✉)
Institute of Chemistry, University of Bialystok, Hurtowa 1, 15-399 Bialystok, Poland
e-mail: artrat@uwb.edu.pl

L. K. Huynh
International University, Vietnam National University, Ho Chi Minh City, Vietnam

L. K. Huynh · Q. B. Pham · T. N. Truong
Institute for Computational Science and Technology, Ho Chi Minh City, Vietnam

T. N. Truong
Department of Chemistry, Henry Eyring Center for Theoretical Chemistry, University of Utah, 315 S. 1400 E. Rm. 2020, Salt Lake City, UT 84112, USA

Published online: 05 February 2013

Since research progress in alkyl radicals chemistry is severely hampered by the complexity of the combustion systems and the lack of molecular-level understanding of fundamental processes taking place, rate coefficients for reactions with many hydrocarbons, such as C_nH_{2n+2}, are not known. Consequently, the fate of these radicals is not well characterized and knowledge of theirs reaction kinetics has been relatively scarce both experimentally and theoretically. Moreover, most of the available data are provided for a limited temperature range only, whereas for modeling of the combustion of hydrocarbon fuels, kinetic information for the wide temperature range is needed. Thus, accurate kinetic data for different metathesis reactions of a wide range of alky radicals are of importance. A common approach used in nearly all kinetic models is to employ systematic rate estimations for well-defined reaction classes [8, 9]. The simplest way is to approximate all reactions in a given class have the same rate (per reaction site). Of the existing more accurate methodologies, the reaction class transition state theory (RC-TST) [10] extrapolates a known rate constant to that of any arbitrary reaction in the same class using correlations, which are constructed under the transition state theory (TST) framework. The key idea of this application is that reactions in the same class have the same reactive moiety whose chemical bonding changes during the course of the reaction, and thus, they are expected to have similarities in their potential energy surfaces along the reaction pathways/valleys. The group additivity (GA) approach is mainly based on the fact that reaction rates depend primarily on the thermodynamic properties of the involved species, for example, the reactants and the corresponding transition state, and that thermal properties can be predicted on the basis of the assumption of group additivity from ab initio calculations. This approach was successfully applied by Sumathi et al. [11, 12], Allen et al. [13], Sabbe et al. [14–17], and Wang et al. [18, 19]. Another approach, where rate rules are derived from a systematic investigation of sets of reactions within a given reaction class using electronic structure calculations performed at the CBS-QB3 level of theory, was reported by Villano et al. [20, 21]. The survey of the different rate estimation rules, together with their applications, was recently reported by Carstensen and Dean [22].

Successful applications of the RC-TST theory to a number of different reaction classes contributed significantly to progress toward better understanding of complex reaction systems [23–25]. In this study, in an attempt to provide a complete picture of the metathesis reactions with alkyl radicals as H abstracting agents, we applied the RC-TST methodology to derive all parameters for estimating the rate constants of any reaction belonging to the $\cdot C_2H_5$ +alkane $\rightarrow$ $\cdot C_2H_6$ + alkyl reaction class. This is done by first deriving the analytical correlation expressions for rate constants of the reference reaction with those in a small representative set of the class from explicit DFT calculations of rate constants for all reactions in this representative set. The assumption is that these correlation expressions can be extended to all reactions in the class. So far, this assumption has been shown to be valid for different reaction families [10, 23–29].

To develop RC-TST/linear energy relationship (LER) parameters for the title reaction family, the representative set consists of 19 reactions as shown below.

$(R_1)p$	Ethane + ethyl → Ethyl + ethane
$(R_2)p$	Propane → 1-propyl
$(R_3)s$	Propane → 2-propyl
$(R_4)p$	Butane → 1-butyl
$(R_5)s$	Butane → 2-butyl
$(R_6)p$	2-methylpropane → 2-methyl-1-propyl
$(R_7)t$	2-methylpropane → 2-methyl-2-propyl
$(R_8)s$	Pentane → 1-pentyl
$(R_9)p$	Pentane → 2-pentyl
$(R_{10})t$	Pentane → 3-pentyl
$(R_{11})s$	2-methylbutane → 2-methyl-1-butyl
$(R_{12})p$	2-methylbutane → 2-methyl-2-butyl
$(R_{13})s$	2-methylbutane → 3-methyl-2-butyl
$(R_{14})s$	2-methylbutane → 3-methyl-1-butyl
$(R_{15})p$	2,2-dimethylpropane → 2,2-dimethyl-1-propyl
$(R_{16})t$	Hexane → 1-hexyl
$(R_{17})p$	Hexane → 2-hexyl
$(R_{18})t$	Hexane → 3-hexyl
$(R_{19})s$	2-methylpentane → 4-methyl-1-pentyl

R_1 is the reference reaction. Among these, eight reactions are at primary C atom (type p), seven others are at secondary carbon (type s), and the four remaining are at tertiary site (type t). Note that the training set does not contain cyclic alkanes. The validity of the derived LER for cyclic alkanes is used as a test on the extendibility of the RC-TST methodology.

2 Methodology

2.1 Reaction class transition state theory

Because the details of the RC-TST method have been presented elsewhere [30], we discuss only its main features here. It is based on the realization that reactions in the same class have the same reactive moiety; thus, the difference between the rate constants of any two reactions is mainly

due to differences in the interactions between the reactive moiety and their different substituents. Within the RC-TST framework, the rate constant of an arbitrary reaction (denoted as k_a) is proportional to that of a reference reaction k_r. Usually, one often would choose the reference reaction to be the smallest reaction in the class, which is referred to as the principal reaction. Any particular reaction in the same class is obtained by extrapolating k_r with a temperature-dependent function *f(T)*:

$$k_{\mathrm{a}}(T) = f(T) \times k_{\mathrm{r}}(T) \tag{1}$$

One often would choose the reference reaction to be the smallest reaction in the class, since their rate constants can be calculated accurately from first principles. The key idea of the RC-TST method is to factor $f(T)$ into different components under the TST framework:

$$f(T) = f_{\sigma} \times f_{\kappa}(T) \times f_{Q}(T) \times f_{V}(T) \times f_{HR}(T) \tag{2}$$

where $f_{textσ}$, f_{κ}, f_{Q}, f_{V}, and f_{HR} are the symmetry number, tunneling, partition function, potential energy, and hindered rotations factors, respectively. These factors are simply the ratios of the corresponding components in the TST expression for the two reactions:

$$f_{\sigma} = \frac{\sigma_{\mathrm{a}}}{\sigma_{\mathrm{r}}} \tag{3}$$

$$f_{\kappa}(T) = \frac{\kappa_{\mathrm{a}}(T)}{\kappa_{\mathrm{r}}(T)} \tag{4}$$

$$f_{\mathrm{Q}}(T) = \frac{\left(\frac{Q_{\mathrm{a}}^{\neq}(T)}{\Phi_{\mathrm{a}}^{R}(T)}\right)}{\left(\frac{Q_{\mathrm{r}}^{\neq}(T)}{\Phi_{\mathrm{r}}^{R}(T)}\right)} = \frac{\left(\frac{Q_{\mathrm{a}}^{\neq}(T)}{Q_{\mathrm{r}}^{\neq}(T)}\right)}{\left(\frac{\Phi_{\mathrm{a}}^{R}(T)}{\Phi_{\mathrm{r}}^{R}(T)}\right)} \tag{5}$$

$$f_{\mathrm{V}}(T) = \exp\left[-\frac{(\Delta V_{\mathrm{a}}^{\neq} - \Delta V_{\mathrm{r}}^{\neq})}{k_{\mathrm{B}}T}\right] = \exp\left[-\frac{\Delta\Delta V^{\neq}}{k_{\mathrm{B}}T}\right] \tag{6}$$

$$f_{\mathrm{HR}}(T) = \frac{c_{\mathrm{HR,a}}(T)}{c_{\mathrm{HR,r}}(T)} \tag{7}$$

where κ(T) is the transmission coefficient accounting for the quantum mechanical tunneling effects; σ is the reaction symmetry number; $Q^{\neq}$ and Φ^{R} are the total partition functions (per unit volume) of the transition state and reactants, respectively; $\Delta V^{\neq}$ is the classical reaction barrier height; c_{HR} symbolizes the correction to the total partition function due to the hindered rotation treatment; T is the temperature in kelvin; k_{B} and h are the Boltzmann and Planck constants, respectively. Among these, only symmetry factor can be easily calculated from the molecular topology of the reactant. Obtaining exact value of four other factors requires structures, energies, and vibrational frequencies of the reactant and transition state for the reaction investigated. The potential energy factor can be calculated using the reaction barrier heights of the arbitrary reaction and the reference reaction. The RC-TST/LER method uses the linear energy relationship (LER) similar to the well-known Evans–Polanyi linear free-energy relationship between classical barrier heights and reaction energies of reactions to estimate reaction barriers and determines the pre-exponential factor (relative to a well-characterized reference reaction) by performing a cost-effective molecular mechanics or DFT calculation with statistical analysis. RC-TST/LER rate constants are estimated using only reaction energy and reactants topology information; no transition state and frequency calculation are needed. This feature makes RC-TST/LER method applicable to the different automated mechanisms generation (ARMG) schemes [1, 31].

2.2 Computational details

All the electronic structure calculations were carried out using the GAUSSIAN 09 suite of programs [32]. Previous applications of RC-TST, hybrid non-local density functional theory (DFT), particularly Becke's half-and-half (BH&H) non-local exchange, and Lee–Yang–Parr (LYP) non-local correlation functional, have been found to be sufficiently accurate for predicting the transition state properties for different classes of reactions [24, 27–29]. Recently, there have been a number of new DFT functional developments, such as the non-local M062X functional [33], designed especially for the chemical kinetics purposes. It would be of great interest to determine whether RC-TST parameters are sensitive to the choice of DFT functional. For this reason, in this study, we employ also the M062X DFT functional in addition to the BH&HLYP one. A discussion on the differences in the final results on the choice of DFT functional is presented further in this study in Sect. 3.4.4.

Geometries of reactants, transition states, and products were thus optimized at the M062X level of theory with the Dunning's correlation-consistent polarized valence double-zeta basis set [3*s*2*p*1*d*/2*s*1*p*] denoted as cc-pVDZ, which is sufficient to capture the physical change along the reaction coordinate for this type of reaction. All reported results for stable molecules as well as transition states were obtained for the lowest energy conformer of a given species. Normal mode analysis was performed at each stationary point to ensure its characteristics, that is, stable structure has zero imaginary vibrational frequency, whereas transition state (TS) structure has one imaginary vibrational frequency, whose mode corresponds to the reaction coordinate of the reaction being considered. Geometry, energy, and frequency information were used to derive the RC-TST factors. The AM1 semiempirical method was also employed to calculate the reaction energies of the reactions considered here. M062X/cc-pVDZ and AM1 reaction energies were then used to derive the LER's between the barrier

heights and the reaction energies. Note that AM1 reaction energy is only used to extract an accurate barrier height from the LERs; it does not directly involve any rate calculations. Minima were confirmed to have adequate convergence and zero imaginary vibrational frequencies. The TS structure was confirmed to have one imaginary vibrational frequency and furthermore shown to be connected to the desired reactant and product by displacement along the normal coordinate for the imaginary vibrational frequency in the positive and negative directions.

To derive the RC-TST correlation functions, TST/Eckart rate constants for all reactions in the above representative reaction set were calculated by employing the TheRate program [34]. In these calculations, overall rotations were treated classically, and vibrations were treated quantum mechanically within the harmonic approximation except for the modes corresponding to the internal rotations of the $-CH_3$ groups, which were treated as the hindered rotations (HRs) using the method suggested by Ayala et al. [35]. Thermal rate constants were calculated for the temperature range of 300–3,000 K, which is sufficient for many combustion applications.

3 Results and discussion

In the section below, we first report on the rate constants for the reference reaction, and then we describe how the RC-TST factors are derived using the training reaction set. Subsequently, we perform three error analyses to provide some estimates of the accuracy of the RC-TST method applied to this reaction class. The first error analysis is the direct comparison between the calculated rate constants with those available in the literature. The second error analysis is a comparison between rate constants calculated by the RC-TST/LER approximation and those from explicit full RC-TST calculations for the whole set. To assess reliability and validity of the correlations, a set of structurally different alkyl radicals, not present in the training set, was also used for this analysis. Final analysis is on the systematic errors from using fitted analytical expressions for the RC-TST/LER correlation functions.

3.1 Reference reaction

The first task for using the RC-TST method is determination of thermal rate constants of the reference reaction. In our previous studies [23, 26, 27], we suggested the use of the smallest reaction, that is, the principal reaction (PR) of the class, to be the reference reaction since its rate constants can be calculated accurately from first principles or are often known experimentally. However, we found that the principal reaction is not always the best reference reaction, and it is also true here. In fact, the hydrogen abstraction by ethyl radical from ethane, $C_2H_6 + \cdot C_2H_5 \rightarrow \cdot C_2H_5 + C_2H_6$, is a better reference reaction than the principal $CH_4 + \cdot C_2H_5 \rightarrow \cdot CH_3 + C_2H_6$ reaction for the following reasons. Although methane is the simplest hydrocarbon, it is known to have unusual stability compared to larger saturated hydrocarbons due to its symmetry and its lack of a C–C bond. In fact, LER for the title reaction class, presented in Sect. 3.2.1, confirms this behavior by showing the barrier of the $CH_4 + \cdot C_2H_5 \rightarrow \cdot CH_3 + C_2H_6$ (principal) reaction does not follow the LER trend as other reactions. For this reason, further discussion is based on the use of the reaction between ethyl and ethane as the reference reaction.

3.1.1 *Potential energy surface*

The optimized geometrical parameters of the reactants and the TS of the $C_2H_6 + \cdot C_2H_5 \rightarrow \cdot C_2H_5 + C_2H_6$ reaction at the M062X/cc-pVDZ level of theory are shown in Fig. 1. The TS was confirmed by normal mode analysis to have only one imaginary frequency whose mode corresponds to the transfer of the hydrogen atom between C_2H_6 and $\cdot C_2H_5$ structures. For the sake of comparison, previously reported values obtained at the MC-QCISD/3 level of theory are also presented [36]. Results demonstrate that both the simple M062X/cc-pVDZ and the rather high-level MC-QCISD/3 methods predict similar geometries for the transition state.

The zero point energy-corrected barrier heights with and without zero point correction (ZPE), calculated at various levels of theory, are listed in Table 1. Dybala-Defratyka et al. [36] carried out a series of high-level calculations

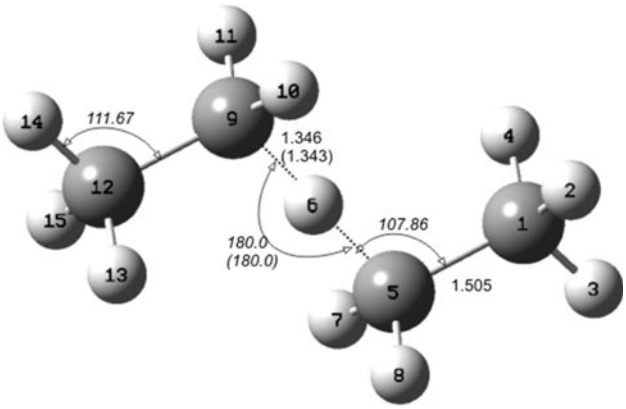

Fig. 1 Optimized geometry (distances in angstroms and angles in degrees) of the transition state of the $C_2H_6 + \cdot C_2H_5 \rightarrow \cdot C_2H_5 + C_2H_6$ reaction at the M062X/cc-pVDZ level of theory (angles are marked as *italics*). The *numbers* in *parentheses* are taken from ref [36]

and suggested the consensus value of 16.7 kcal/mol for the classical barrier. The M062X/cc-pVDZ barrier of 16.3 kcal/mol is in good agreement with this value, while the BH&HLYP/cc-pVDZ barrier of 18.2 kcal/mol is noticeably higher. Using the larger basis set such as the cc-pVTZ only improves the agreement for both functionals slightly. The compound method CBS-QB3 is expected to yield the most accurate ZPE-corrected barrier height, specifically 15.0 kcal/mol. The best agreement with the CBS-QB3 value is M062X/cc-pVDZ value of 15.1 kcal/mol, and the worst is BH&HLYP/cc-pVDZ value of 17.1 kcal/mol. Consequently, M062X/cc-pVDZ is used to obtain the energies and hessians along the minimum energy path (MEP) of the reference reaction as well as all RC-TST parameters, while BH&HLYP/cc-pVDZ is used to study the sensitivity of RC-TST parameters on the choice of DFT functional.

The classical the vibrationally adiabatic ground-state potential curve V_g^a, which is the sum of the two terms V_C + ZPE, is illustrated in Fig. 2, relative to its reactant values. As may be seen from Fig. 2, the ZPE correction lowers the classical barrier height about 1.2 kcal/mol, which corresponds to 7–8 %. The separation of the two maxima of the $V_C(s)$ and $V_g^a(s)$ curves reflects the extent of the variational effect for the calculation of rate constants. Figure 2 shows they are nearly the same, thus implies that the variational effects are small for the reference reaction. The classical adiabatic ground-state potential V_C curves for reactions R_1-R_4 are given in the Supporting Info file (Figure S_1).

3.1.2 Rate constants

Thermal rate constants of the reference reaction were calculated using the canonical variational transition state theory (CVT) with small curvature tunneling (SCT) corrections. In addition, to model vibrations transverse to the reaction path, we used curvilinear coordinates based on bond stretches, valence angle bends, and bond torsions as implemented in the POLYRATE 2010a program [37]. Harmonic vibrational frequencies were calculated at 200 selected points (100 points in the reactant channel and 100 points in the product channel) along the MEP. However, since the MEP is symmetric, actual calculations were only done for 100 points on the reactant side. According to the methodology detailed in Ref. [38], a reaction symmetry number of 6 was used to account for the number of symmetrically equivalent reaction paths. The low-frequency modes correspond to rotations of the $-CH_3$ groups in the reactants and transition states are treated as hindered rotors. The final CVT/SCT/HR rate constants are plotted in Fig. 3 and fitted to an Arrhenius expression, given as:

Table 1 Calculated classical (V_C) and zero point corrected (V_g^a) barriers height for the $C_2H_6 + \cdot C_2H_5 \rightarrow \cdot C_2H_5 + C_2H_6$ reaction (numbers are in kcal/mol)

Level of theory	Classical barrier V_c	Zero point corrected barrier V_g^a
BH&HLYP(CC-pVDZ)	18.2	17.1
BH&HLYP (CC-pVTZ)	17.9	16.8
B3LYP/cc-pVDZ	14.3	13.1
B3LYP/cc-pVTZ	16.3	15.1
B3LYP/6-31 + G(d,p) [36]	15.8	–
M052X/cc-pVDZ	15.0	13.6
M052X/cc-pVTZ	16.5	15.2
M052X/CBSB7	16.0	14.8
M062X/cc-pVDZ	16.3	15.1
M062X/cc-pVTZ	17.2	16.1
CBS-QB3	16.1	15.0
CBS-Q//MP2/6-31G(d†) [36]	15.8	–
CCSD(T)/cc-pVDZ//M062X/cc-pVDZ	15.4	14.2
MP2/cc-pVDZ//M062X/cc-pVDZ	15.6	14.5
MP2/cc-pVTZ//M062X/cc-pVDZ	17.1	15.9
MP2/CBSB7//M062X/cc-pVDZ	16.9	15.8
MP4/cc-pVDZ//M062X/cc-pVDZ	15.4	14.3
MP4/cc-pVTZ//M062X/cc-pVDZ	16.4	15.2
MP4/CBSB7//M062X/cc-pVDZ	16.1	15.0
G3S//MP2(full)/6-31G(d) [36]	16.3	–
G3SX(MP3)//B3LYP/6-31G(2df,p) [36]	16.5	–
Consensus barrier heights [36]	16.7	–

$$k_r(T) = (2.34 \times 10^{-24}) T^{3.54} \exp\left(\frac{-4564}{T}\right) (\mathrm{cm^3\ s^{-1}\ molecule^{-1}}) \quad (8)$$

Note that the small difference between TST and CVT results confirms the earlier expectation of small variational effects in this reaction. Furthermore, differences in CVT and CVT/SCT rate constants indicate a rather significant tunneling contribution at low temperatures.

Although the reaction set is an important part of the series of Lawrence Livermore National Laboratory (LLNL) mechanisms [8, 9], the reference reaction is not included in these models. To the best of our knowledge, there have not been any reports on the rates of the reference reaction.

3.2 Reaction class parameters

This section describes how the RC-TST factors were derived using the representative reaction set.

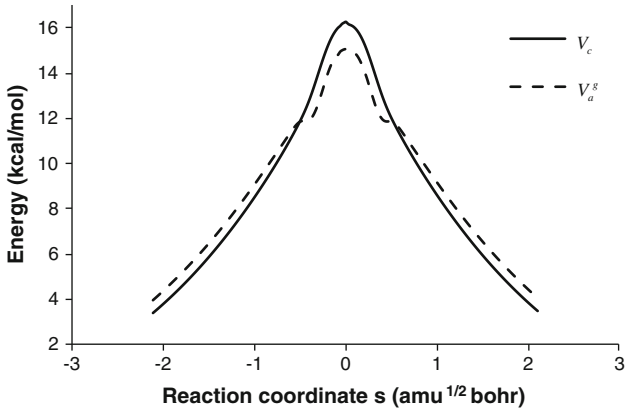

Fig. 2 Potential energy curves along the reaction coordinates of the $C_2H_6 + \cdot C_2H_5 \rightarrow \cdot C_2H_5 + C_2H_6$ reaction. V_g^a is the vibrationally adiabatic ground-state potential curve, and V_C is the classical adiabatic ground-state potential curve

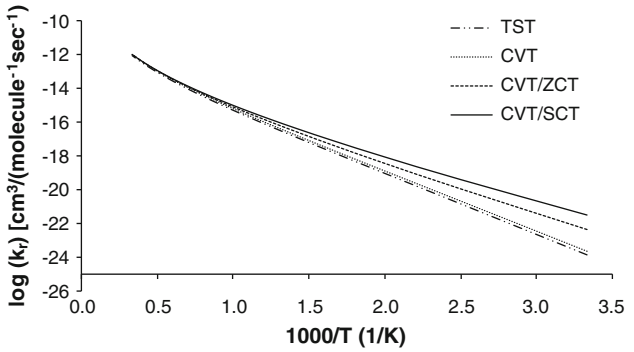

Fig. 3 Arrhenius plot of the calculated rate constants for the $C_2H_6 + \cdot C_2H_5 \rightarrow \cdot C_2H_5 + C_2H_6$ reaction

3.2.1 *Potential energy factor*

The potential energy factor can be calculated using Eq. 6, where $\Delta V_a^{\neq}$ and $\Delta V_r^{\neq}$ are the barrier heights of the arbitrary and reference reactions, respectively. It has been shown previously that within a given class, there is a linear energy relationship (LER) between the barrier height and the reaction energy, similar to the well-known Evans–Polanyi linear free-energy relationship. Thus, with a LER, accurate barrier heights can be predicted from only the reaction energies. In this study, the LER is determined, where the reaction energy can be calculated by either the AM1 or the M062X level of theory. The reaction energies and barrier heights for all reactions in the representative set are given explicitly in Table 2. The observed LER's plotted against the reaction energies calculated at the M062X/cc-pVDZ and AM1 levels are shown in Fig. 4a, b. Note that as mentioned earlier, the principal reaction $CH_4 + \cdot C_2H_5 \rightarrow \cdot CH_3 + C_2H_6$ does not follow the same LER trend as other reaction in this class as illustrated in Fig. 4a as data point PR. Consequently, it is not included in the LER analysis. The linear fits obtained with the least-squares fitting method have the following expressions:

$$\Delta V_a^{\neq} = 0.67 \times \Delta E^{\mathrm{M062X}} + 15.9\,(\mathrm{kcal/mol}) \quad (9a)$$

$$\Delta V_a^{\neq} = 0.39 \times \Delta E^{\mathrm{AM1}} + 15.8\,(\mathrm{kcal/mol}) \quad (9b)$$

The absolute deviations of reaction barrier heights between the LERs and the direct DFT M062X/cc-pVDZ calculations are smaller than 0.4 kcal/mol (see Table 2). The mean absolute deviations of reaction barrier heights predicted from M062X and AM1 reaction energies are 0.21 and 0.27 kcal/mol, respectively. These deviations are, in fact, smaller than the systematic errors of the computed reaction barriers from full electronic structure calculations (see Table 1). This is certainly an acceptable level of accuracy for kinetic modeling. Note that in the RC-TST/LER methodology, only the relative barrier height is needed. To compute these relative values, the barrier height of the reference reaction R_1 calculated at the same level of theory, that is, M062X/cc-pVDZ, is needed and has the value of 16.30 kcal/mol (see Table 2).

Alternatively, it is possible to approximate all reactions at the same type of carbon atom site as having the same barrier height, namely the average value. In previous studies, this approximation was referred to as the barrier height grouping (BHG) approximation. It was shown that substitution of an alkyl group stabilizes the radical species, thus lowering the barrier height. Thus, one can expect hydrogen abstractions reactions from the tertiary carbon to have lower barrier height than those from a secondary carbon. The same relationship is expected to hold between H abstractions from a secondary and primary carbon atom. These expectations were confirmed in our DFT calculations, when the average barrier heights for H abstractions from a primary, secondary, and tertiary carbon were 16.00, 13.85 and 12.37 kcal/mol, respectively. The averaged deviations of reaction barrier heights estimated from grouping are 0.35, 0.18 and 0.10 kcal/mol, respectively, which correspond to 2.2, 1.3 and 0.8 % of the mean barrier height. Therefore, this approach can also be used to estimate the relative barrier height quickly with an acceptable, that is, less than 3 %, deviation. The key advantage of this approach is that it does not require any addition information to estimate rate constants.

In conclusion, the barrier heights for any reaction in this reaction class can be obtained by using either the LER or BHG approach. The estimated barrier height is then used to calculate the potential energy factor using Eq. (6). The performance for such estimations on the whole representative reaction set is discussed in the error analyses below.

Table 2 Classical reaction energies, barrier heights, and absolute deviations between calculated barrier heights from DFT and semiempirical calculations and those from LER expressions and BHG approach

Reaction	ΔE		$\Delta V^{\neq}$				$\left\lvert \Delta V^{\neq} - \Delta V^{\neq}_{estimated} \right\rvert$[f]		
	DFT[a]	AM1[b]	DFT[a]	DFT[c]	AM1[d]	BHG[e]	DFT[c]	AM1[d]	BHG[e]
R_1	0.00	0.00	16.30	15.91	15.82	16.00	0.38	0.48	0.29
R_2	0.48	1.02	16.38	16.23	16.21	16.00	0.14	0.16	0.37
R_3	−3.26	−5.26	14.11	13.74	13.75	13.85	0.36	0.36	0.26
R_4	0.20	0.12	15.74	16.04	15.86	16.00	0.30	0.12	0.26
R_5	−2.99	−5.03	13.75	13.92	13.84	13.85	0.18	0.09	0.10
R_6	0.72	0.69	16.34	16.39	16.09	16.00	0.05	0.26	0.34
R_7	−5.62	−9.67	12.56	12.17	12.02	12.37	0.39	0.54	0.19
R_8	−3.05	−5.06	13.67	13.88	13.83	13.85	0.21	0.16	0.18
R_9	0.62	0.71	15.97	16.32	16.09	16.00	0.35	0.13	0.04
R_{10}	−5.26	−9.46	12.31	12.41	12.10	12.37	0.10	0.21	0.06
R_{11}	−3.11	−4.63	13.62	13.84	14.00	13.85	0.23	0.38	0.23
R_{12}	−0.65	−0.08	15.36	15.48	15.78	16.00	0.12	0.43	0.65
R_{13}	−3.05	−5.05	14.02	13.88	13.83	13.85	0.14	0.19	0.18
R_{14}	−2.84	−4.70	13.72	14.02	13.97	13.85	0.30	0.25	0.13
R_{15}	0.42	0.12	16.40	16.19	15.86	16.00	0.20	0.53	0.39
R_{16}	−5.32	−8.49	12.33	12.37	12.48	12.37	0.04	0.15	0.04
R_{17}	−1.09	0.48	15.54	15.19	16.01	16.00	0.35	0.47	0.46
R_{18}	−5.08	−9.32	12.29	12.53	12.16	12.37	0.24	0.14	0.08
R_{19}	−3.01	−5.05	14.04	13.91	13.83	13.85	0.14	0.21	0.20
MAD[g]							**0.20**	**0.27**	**0.23**

Zero point energy correction is not included. Energies are in kcal/mol

[a] Calculated at M062X/cc-pVDZ level of theory

[b] Calculated at AM1 level of theory

[c] Calculated from the LER using reaction energies calculated at M062X/cc-pVDZ level of theory: Eq. (9a)

[d] Calculated from the LER using reaction energies calculated at AM1 level of theory: Eq. (9b)

[e] Estimated from barrier height grouping

[f] $\Delta V^{\neq}$ from M062X/cc-pVDZ calculations; $\Delta V^{\neq}_{\text{estimated}}$ from the linear energy relationship using M062X/cc-pVDZ and AM1 reaction energies or from barrier height grouping

[g] Medium absolute deviations (MAD) for reactions R_2–R_{19}

3.2.2 *Reaction symmetry number factor*

The reaction symmetry number factors f_σ were calculated simply from the ratio of reaction symmetry numbers of the arbitrary and reference reactions using Eq. 3 and are listed in Table 3. The reaction symmetry number of a reaction is given by the number of symmetrically equivalent reaction paths. For the title reaction class, this number is the product of the number of H atoms connected to the hydrogen abstraction site (three for primary carbons, two for secondary, and one for tertiary) and the number of equivalent abstraction sites in the molecule. Since there are two equivalent primary C atoms in all the n-alkanes molecules, the reaction symmetry number is equal to $2 \times 3 = 6$. This number may increase for branched alkanes, however. For example, it is equal to $4 \times 3 = 12$ for reactions R_{3A} and R_{9A}, where four equivalent methyl groups exist in the reagent molecule. In any case, this value can be easily calculated from the molecular topology of the reactant; thus, the symmetry number factor can be calculated exactly.

3.2.3 *Tunneling factor*

It is well known that tunneling is of great importance for the light particles transfer [28, 39–48]. As may be seen from Fig. 3, it is also important for the reference reaction of the title reaction class. The tunneling factor f_κ, which captures the changes of the tunneling magnitude from reference reaction to other processes within the reaction family, is defined as a ratio of the transmission coefficient of reaction R_a to that of the reference reaction R_r

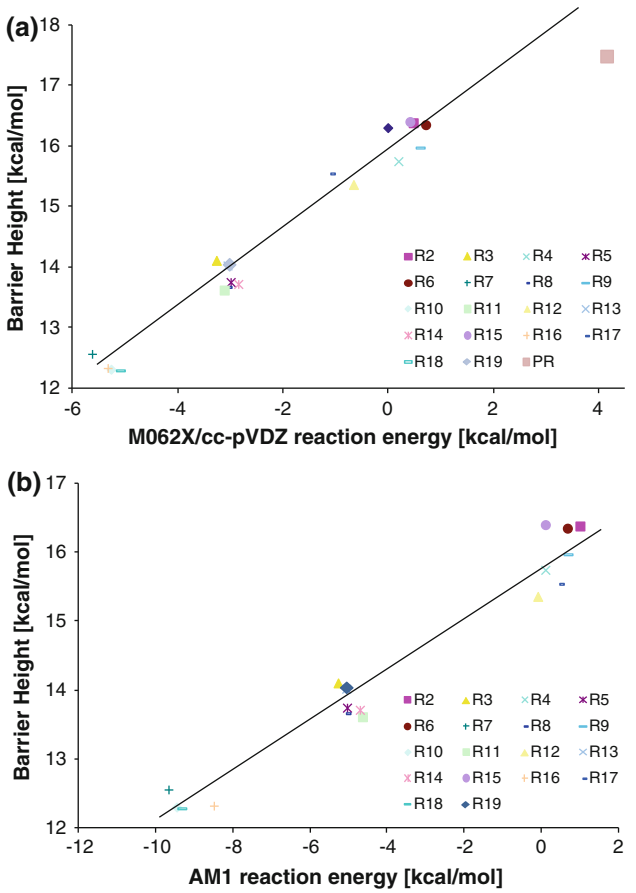

Fig. 4 Linear energy relationship plot of the barrier heights, $\Delta V^{\neq}$, versus the reaction energies, ΔE. Barrier heights were calculated at the M062X/cc-pVDZ level of theory. ΔE's were calculated at **a** the M062X/cc-pVDZ and **b** AM1 level of theory

(see Eq. 4). It is important to point out that factor f_κ is the scaling factor for scaling the tunneling coefficient which can be calculated with an accurate multi-dimensional tunneling method or is implicit from experimental data of the reference reaction to that of the reaction of interest. This scaling factor can be estimated using the one-dimension Eckart method. The validity of such an approximation for the hydrogen transfer processes was examined in our previously study [30], where f_κ was calculated from explicit multidimensional tunneling calculations and compared to those from Eckart calculations. The resulting differences were found to be less than 34 % at the room temperature for the entire test cases where tunneling was known to be significant. The differences are smaller at larger temperatures. This is due to the cancelation of errors by using the Eckart model in calculations of the tunneling factors. Since our interest is in providing kinetic data for combustion modeling where the lower temperature limit is at the room temperature, thus the use of Eckart model for obtaining the tunneling factor is sufficient.

Calculated results for the representative reaction set are fitted to an analytical expression. It is known that the tunneling coefficient depends on the barrier height. We have shown that the barrier heights group together into three groups, namely primary, secondary, and tertiary carbon site (see the Sect. 3.2.1); thus, it is expected that reactions in the same group have similar tunneling factors and the average value can be used for the whole group.

For the title reaction class, tunneling effect was found to be very similar for primary and secondary hydrogen abstraction sites; thus, only two correlations are needed. Simple expressions for the tunneling factors for primary–secondary and tertiary carbon sites were obtained by fitting to the average calculated values and are given below:

$$f_{\kappa,prim-\mathrm{sec}} = 1 - 1.71 \times \exp\left(-77.81/T\right) \quad \text{(10a)}$$

for primary and secondary carbon sites

$$f_{\kappa,tert} = 1 - 5.26 \times \exp\left(-91.84/T\right) \quad \text{(10b)}$$

for tertiary carbon sites.

Two above equations are plotted in Fig. 5, and the error analysis at 300 K is listed in Table 3. It can be seen that the same tunneling factor expression can be reasonably assigned to all reactions at the same site with the largest percentage deviation of 11.3 % for R_7 and R_{10}; the mean absolute deviation is equal to 5.7 %, as compared to the direct Eckart calculations. At higher temperatures, tunneling contributions to the rate constants decrease, and thus, as expected, the differences between the approximated values and the explicitly calculated ones also decrease; the maximum error for all reactions is less than 1 % at 600 K.

3.2.4 *Partition function factor*

The partition factor is the product of the translational, rotational, internal rotation, vibrational, and electronic component. The translational and rotational factors are temperature independent. As pointed out in our previous study [26], the temperature-dependent part of the total partition function factor f_Q mainly originates from the differences in the coupling between the substituents with the reactive moiety and its temperature dependence, which arises from the vibrational component and internal rotations only. Note that because contributions from the HR (hindered rotors) modes are treated separately, they are not included in these partition function calculations. The average values of partition function factors for primary, secondary, and tertiary carbon abstraction sites were calculated in the temperature range of 300–3,000 K. Since plots of these factors are nearly temperature independent, they were fitted into the constant expressions as given below:

Table 3 Calculated symmetry number factors and tunneling factors at 300 K

Reaction	Symmetry number factor	Tunneling ratio factor, f_κ			
		Eckart[a]	Fitting[b]	Deviation[c]	% Deviation[d]
R_1	1.00	(248)[f]	–	–	–
R_2	1.00	0.93	0.96	0.04	4.0
R_3	0.33	0.89	0.97	0.08	9.2
R_4	1.00	1.02	0.96	0.05	5.3
R_5	0.67	0.94	0.97	0.03	2.8
R_6	1.00	1.01	0.96	0.05	4.5
R_7	0.17	0.87	0.96	0.10	11.3
R_7	0.67	0.94	0.97	0.03	2.8
R_9	0.50	0.91	0.96	0.05	5.5
R_{10}	0.17	0.72	0.80	0.08	11.3
R_{11}	0.33	1.02	0.97	0.05	4.8
R_{12}	0.50	1.02	0.96	0.05	5.1
R_{13}	0.67	1.00	0.97	0.03	3.1
R_{14}	0.67	1.01	0.97	0.04	4.4
R_{15}	0.50	0.94	0.96	0.03	2.7
R_{16}	0.17	0.74	0.80	0.06	7.6
R_{17}	0.50	0.93	0.96	0.04	4.1
R_{18}	0.33	0.86	0.80	0.07	7.8
R_{19}	0.67	1.01	1.00	0.01	0.9
MAD[e]				**0.05**	**5.7**

[a] Calculated directly using Eckart method with M062X/cc-pVDZ reaction barrier heights and energies

[b] Calculated by using fitting expression

[c] Absolute deviation between the fitting and directly calculated values

[d] Percentage deviation (%)

[e] Medium absolute deviations (MAD) and deviation percentage between the fitting and directly calculated values

[f] Tunneling coefficient calculated for reaction (R_1) using the Eckart method with the energetic and frequency information at M062X/cc–pVDZ

$$f_{Q,\mathrm{pri}} = 0.74 \quad \text{for primary carbon sites} \tag{11a}$$

$$f_{\mathrm{sec},tert} = 0.62 \quad \text{for secondary and tertiary carbon sites} \tag{11b}$$

As one may see from Eqs. 11a, b, the average value of partition function factor differs from unity. As mentioned earlier, the coupling between substituents with the reactive moiety is believed to account for these differences.

3.2.5 HR factor

It is important to point out that the motion of the internal rotation of the methyl group in the reactive moiety, internal rotors gain and loss in the course of the reaction, and contributions from different transition state rotational

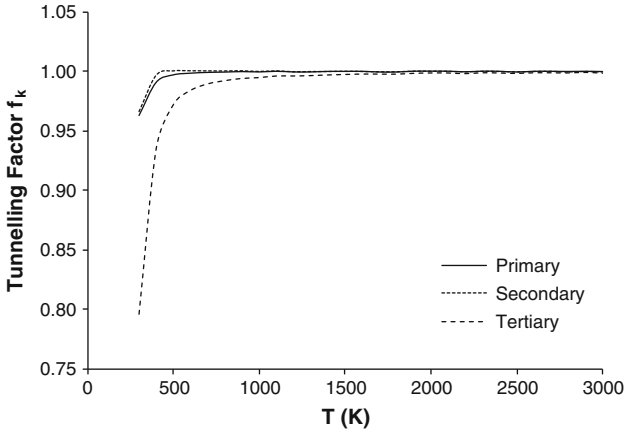

Fig. 5 Plots of the tunneling ratio factors f_κ as functions of the temperature for the $C_2H_5\cdot$ + alkane → C_2H_6 + alkyl reaction class from primary, secondary, and tertiary carbon sites

conformers are already treated explicitly in the rate constants of the reference reaction $C_2H_6 + \cdot C_2H_5 \rightarrow \cdot C_2H_5 + C_2H_6$. Thus, the reaction class factor due to these hindered rotations is a measure of the substituent effects on the rate constant from the hindered rotors *relative* to that of the reference reaction R_1. We used the approach proposed by Ayala and Schlegel [35] to calculate the hindered rotation correction factor to the partition function for a certain vibrational mode. In this case, the rotating group, the periodicity number of the torsional potential of the vibrational mode, geometry of the molecule is needed. Previous study by Kungwan and Truong [23] shows that, for the $CH_3\cdot$ + alkane → CH_4 + alkyl reaction class, relative contribution of hindered rotations from alkyl groups larger than CH_3 is small due to the cancelation occurred within the RC-TST framework. Similar situation is expected for the title reaction class; thus, we consider hindered rotation treatment for the $–CH_3$ in this study. We found that the rotational potential barriers depend slightly on the type of the carbon atom to which the methyl group is directly connected. These barriers were calculated to be of 3.3, 3.5, and 3.9 kcal/mol for the $–CH_3$ groups bonded to secondary, tertiary, and quaternary sp^3 C atoms, respectively. Within any of these sets, differences in the barriers were found to be negligible, that is, less than 0.3 kcal/mol. The potential energy curves for both of these kinds of internal rotations are plotted in the Figure S_2 in the Supporting Info. Consequently, the HR factor differs for these sites. The effect of the hindered rotation treatment to total rate constants can be seen in Fig. 6. Individual factors for particular reactions R_2–R_{19}, tantamount to the k_{HO}/k_{HR} values for these reactions, are listed in the Table S_2 of the Supporting Info. It can be seen from Fig. 6 that the average HR factor is temperature dependent, approaching 1 in the low (vibrator) and decreasing below 1 in the high (free rotors) temperature

regimes. There is an observable difference between factors for primary and other H abstraction sites; this trend is clearly related to branching. Its value is fitted to analytical expressions as given below:

$$f_{\mathrm{HR,primary}} = 8.41 \times 10^{-11}T^3 + 4.86 \times 10^{-7}T^2 - 6.62 \times 10^{-4}T + 1.01 \quad (12a)$$

$$f_{\mathrm{HR,secondary}} = 9.72 \times 10^{-11}T^3 + 5.52 \times 10^{-7}T^2 + 7.31 \times 10^{-4}T + 1.07 \quad (12b)$$

$$f_{\mathrm{HR,tertiary}} = 1.05 \times 10^{-10}T^3 + 6.35 \times 10^{-7}T^2 + 9.97 \times 10^{-4}T + 0.93. \quad (12c)$$

3.3 Prediction of rate constants

What we have established so far are the necessary parameters, namely potential energy factor, reaction symmetry number factor, tunneling factor, and partition function factors for the application of the RC-TST theory to predict rate constants for any reaction in the hydrogen abstraction by the ethyl radical reaction class. The procedure for calculating rate constants of an arbitrary reaction in this class is to: (1) calculate the potential energy factor using Eq. 6 with the barrier of the reference reaction of 16.30 kcal/mol. The reaction barrier height can be obtained by using the LER approach by employing Eq. 9a for M062X/cc-pVDZ or Eq. 9b for AM1 reaction energies or by the BHG approach; (2) calculate the symmetry number factor from Eq. 3 or see Table 3; (3) compute the tunneling factor using Eqs. 10a, b) for primary, secondary, and tertiary carbon sites, respectively; (4) evaluate the partition function factor using Eqs. 11a, b); (5) evaluate the HR factor using Eqs. 12a–c); and (6) the rate constants of the arbitrary reaction can be calculated by taking the product of the reference reaction rate constant given by Eq. 8 with the reaction class factors above. Table 4 summarizes the RC-TST parameters for this reaction class. Rules presented in this table enable one to obtain any rate constants within the hydrogen abstraction by ethyl radical reaction class. For the reasons discussed in Sect. 3.1, these rules should not be used for the simplest reaction within this class, namely $C_2H_6 + \cdot CH_3 \rightarrow \cdot C_2H_5 + CH_4$. For this reaction, we recommend using rate constants obtained in our previous study, [23] namely

$$k_{C_2H_6+\cdot CH_3 \rightarrow \cdot C_2H_5+CH_4}(T) = (6.20 \times 10^{-27})T^{5.85} \exp\left(\frac{-5438.45}{T}\right)(\mathrm{cm^3\ s^{-1}\ molecule^{-1}}) \quad (13)$$

If the BHG barrier heights and average values for other factors are used, the rate constants are denoted by RC-TST/BHG. The RC-TST/BHG rate constants for any reactions belonging to this class can be estimated without any further calculations as:

$$k_{\mathrm{prim}}(T) = \sigma_a \times 2.6 \times 10^{-25} \times T^{3.76} \times \exp\left(\frac{-4827}{T}\right)(\mathrm{cm^3\ s^{-1}\ molecule^{-1}}) \quad (13a)$$

for primary carbon sites

$$k_{\mathrm{sec}}(T) = \sigma_a \times 2.6 \times 10^{-25} \times T^{3.71} \times \exp\left(\frac{-3301}{T}\right)(\mathrm{cm^3\ s^{-1}\ molecule^{-1}}) \quad (13b)$$

for secondary carbon sites

$$k_{\mathrm{tert}}(T) = \sigma_a \times 2.6 \times 10^{-25} \times T^{3.65} \times \exp\left(\frac{-2540}{T}\right)(\mathrm{cm^3\ s^{-1}\ molecule^{-1}}) \quad (13c)$$

for tertiary carbon sites

In the Eqs. 13a–c, σ_a denotes symmetry number, accounting for the number of equivalent H abstraction sites. It is important to realize the difference between symmetry number here and the symmetry factor, discussed in Sect. 3.2.2. The symmetry factors of one for primary carbon sites, 4/6 for secondary, and 1/6 for tertiary carbon site are already implicitly included in the rate constant expressions above, thus for the majority of processes $\sigma_a = 1$. For some cases, however, the use of these equations for a target reaction requires multiplication with its proper symmetry number $\sigma_a \neq 1$. Among reactions from the training set, reactions R_{3A} and R_{9A} can serve as examples here. Both these processes are of type *p* with four equivalent H abstraction sites. Since there are only two such sites for the reference reaction, the symmetry number σ_a is, for reactions R_{3A} and R_{9A}, equal to 2.

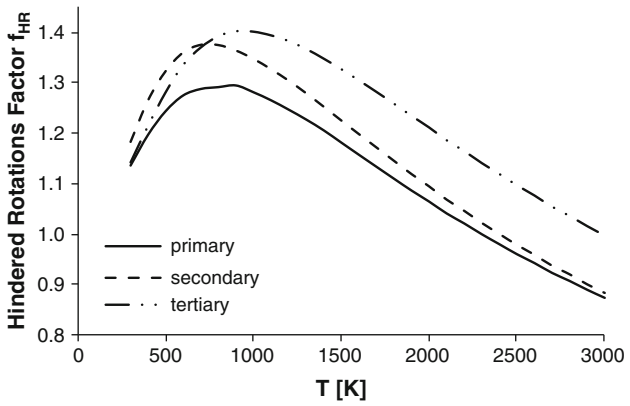

Fig. 6 Plot of the average HR corrections to the total rate constants for all reactions in the temperature range of 300–3,000 K

Table 4 Parameters and formulations of the RC-TST method for the $C_2H_5\cdot$ + alkane → $\cdot C_2H_6$ + alkyl reaction class (C_2H_6 + $\cdot C_2H_5$ → $\cdot C_2H_5$ + C_2H_6 is the reference reaction)

$k_a(T) = k_p(T)\cdot f_k(T)\cdot f_Q(T)\cdot f_{HR}(T)\cdot f_v(T)\cdot f_\sigma$; $f_v(T) = \exp\left[\frac{-(\Delta V^{\neq} - \Delta V_r^{\neq})}{k_B T}\right]$	
T is in kelvin; $\Delta V^{\neq}$ and ΔE are in kcal/mol; zero point energy correction is not included	
f_σ	Calculated explicitly from the symmetry of reactions (see Table 3)
$f_\kappa(T)$	$f_{\kappa,pri-sec} = 1 - 1.71\times\exp\left(-77.81/T\right)$ for primary and secondary carbon sites
	$f_{\kappa,tert} = 1 - 5.26\times\exp\left(-91.84/T\right)$ for tertiary carbon sites
$f_Q(T)$	$f_{Q,pri} = 0.74$ for primary carbon sites
	$f_{sec,tert} = 0.62$ for secondary and tertiary carbon sites
$f_{HR}(T)$	$f_{HR,primary} = 8.41\times10^{-11}T^3 + 4.86\times10^{-7}T^2 - 6.62\times10^{-4}T + 1.01$ for prim. sites
	$f_{HR,secondary} = 9.72\times10^{-11}T^3 + 5.52\times10^{-7}T^2 + 7.31\times10^{-4}T + 1.07$ for sec. sites
	$f_{HR,tertiary} = 1.05\times10^{-10}T^3 + 6.35\times10^{-7}T^2 + 9.97\times10^{-4}T + 0.93$ for tert. sites
$\Delta V^{\neq}$	LER $\Delta V_a = 0.67\times\Delta E^{M062X} + 15.9$ (kcal/mol)
	$\Delta V_a = 0.39\times\Delta E^{AM1} + 15.8$ (kcal/mol)
	$\Delta V_r^{\neq} = 16.30$ kcal/mol
$k_p(T)$	$k_r(T) = (2.34\times10^{-24})T^{3.54}\exp\left(\frac{-4564}{T}\right)$ ($cm^3\ s^{-1}$ molecule^{-1})
BHG approach	$k_{prim}(T) = \sigma_a\times2.6\times10^{-25}\times T^{3.76}\times\exp\left(\frac{-4827}{T}\right)$ ($cm^3\ s^{-1}$ molecule^{-1})
	$k_{sec}(T) = \sigma_a\times2.6\times10^{-25}\times T^{3.71}\times\exp\left(\frac{-3301}{T}\right)$ ($cm^3\ s^{-1}$ molecule^{-1})
	$k_{tert}(T) = \sigma_a\times2.6\times10^{-25}\times T^{3.65}\times\exp\left(\frac{-2540}{T}\right)$ ($cm^3\ s^{-1}$ molecule^{-1})

3.4 Error analyses

3.4.1 Comparisons to experimental data

The first error analysis compares RC-TST results with those from experimental results. As mentioned earlier, very few experimental data are available for the title reaction class. Kinetic data for H abstractions from primary (reactions R_2—Ref. [49] and R_6– Ref. [50]), secondary (reaction R_3—Ref. [49]), and tertiary (reaction R_7—Ref. [50]) carbon atoms in propane and isobutane were reported by Tsang in his extensive literature reviews [49, 50] with uncertainty factor of 2.5, and these data were also used in the LLNL mechanisms [7]. The uncertainty factor defines the range of possible k value of k_m/f and k_m*f, where k_m is the reported value. These results are used to validate rates obtained for reactions from the representative training set, that is, reactions R_2–R_{19}. To test the extendibility of the LER equations to reactions with other alkanes not in the training set such as cycloalkanes or alkanes with aromatic substituents, we used two reactions, namely cyclopentane + $\cdot C_2H_5$ → cyclopentyl + C_2H_6 and toluene + $\cdot C_2H_5$ → benzyl + C_2H_6. Experimental reaction rates for those cyclic systems were previously reported in a number of studies [51–53]. Figure 7a–f shows the predicted rate constants of these reactions using the RC-TST method and from the literature data. In this figure, the "RC-TST LER" notation means that the reaction class factors were calculated with the approximate expressions listed in Table 6. Because there are not significant differences between the results obtained from either using the M062X/cc-pVDZ or using the AM1 reaction energies, only rate constants from M062X are presented here. The agreement between the predicted results and these derived by Tsang for reactions R_2, R_3, R_6, and R_7 is quite excellent—the predicted theoretical data lie within the error bars claimed by Tsang for $T > 600$ K. For the temperatures lower than 600 K, the differences are more noticeable but are still acceptable. It is interesting to note that both RC-TST/LER and RC-TST/BHG work well for these cases. For reactions involving cyclic species (Fig. 7e, f), experimental data agree well with full RC-TST and RC-TST/LER results. As can be seen in Fig. 7e, the RC-TST/BHG approach yields larger errors but are acceptable. As reported previously [24], similar situation also happens for H abstraction by vinyl radical reaction class.

3.4.2 Comparisons to explicit RC-TST calculations

The systematic errors introduced by the LER and BHG approaches are discussed in details in the next error analysis, which compares RC-TST/LER and RC-TST/BHG results with those from explicit calculations. As mentioned in our previous studies [10, 26], the RC-TST methodology can be thought of as a procedure for extrapolating rate constants of the reference reaction to those of any reaction in the class. Comparisons between the calculated rate constants for a small number of reactions using both the RC-TST/LER or RC-TST/BHG and the full RC-TST

methods provide additional information on the accuracy of the LER and BHG approximations. The results for this error analysis for 19 representative reactions (i.e., the comparisons between the RC-TST/LER and full RC-TST methods) are shown in Fig. 8a, wherein the relative deviation defined by $(|k^{\text{RC-TST}} - k^{\text{RC-TST/LER}}|/k^{\text{RC-TST}})$ as a percent versus the temperature for all reactions in the representative set, R_2–R_{19}, is plotted. In Fig. 8, it is important to note the error range, that is, the *y*-range of the collective 19 curves rather than to follow the temperature behavior of one specific curve, that is, reaction. For the temperatures >1,500 K all the reactions in this set, the unsigned relative errors are within 60 %. In the low temperature regime, the errors for all the reactions are still less than 120 %. So, in general, it can be concluded that RC-TST/LER can estimate thermal rate constants for reactions in this class within 100 % when compared to those calculated explicitly using the full RC-TST method. Similar analysis is presented for the RC-TST/BHG approach as shown in Fig. 8b. As expected, RC-TST/BHG has the larger errors, especially in the low temperature regime. Specifically, 2 reactions among 19 show errors larger than 150 %. The accuracy of the BGH approach is noticeable worse than that of the LER approximation, and the convenience of ready to be used rate expressions for any reaction in the class may offset the less accuracy of the BHG compared to LER, however.

To demonstrate the reliability of the correlations, further validation is needed to verify that the 19 reaction representative sets selected for developing the RC-TST/LER parameters are sufficient to represent this reaction class. We calculated the relative deviation defined by $(|k^{\text{RC-TST}} - k^{\text{RC-TST/LER}}|/k^{\text{RC-TST}})$ for 14 additional reactions, not included in the training set. In particular, these reactions are as follows:

(R_{1A})	Pentane + ethyl → 1-pentyl + ethane
(R_{2A})	Pentane → 3-pentyl
(R_{3A})	2,2-dimethylpropane → 2,2-dimethyl-1-propyl
(R_{4A})	Hexane → 1-hexyl
(R_{5A})	2-methylpentane → 4-methyl-2-pentyl
(R_{6A})	2-methylpentane → 2-methyl-3-pentyl
(R_{7A})	2-methylpentane → 2-methyl-1-pentyl
(R_{8A})	2,2-dimethylbutane → 3,3-dimethyl-2-butyl
(R_{9A})	2,3-dimethylbutane → 2,3-dimethyl-1-butyl
(R_{10A})	Heptane → 1-heptyl
(R_{11A})	2,2,4-trimethylpentane → 2,2,4-trimethyl-1-pentyl
(R_{12A})	2,2,4-trimethylpentane → 2,2,4-trimethyl-3-pentyl
(R_{13A})	Toluene → Benzyl
(R_{14A})	Cyclopentane → Cyclopentyl

The results are plotted in Fig. 9. Of the reactions R_{1A}-R_{14A}, those with 2,2,4-trimethyl-1-pentane (isooctane) (reactions R_{11A}–R_{12A}), which are currently used to model branched alkanes in diesel fuel surrogates, are of particular interest to the combustion community. As can be seen from Fig. 9, kinetic data for these H abstraction by ethyl radical from highly branched alkyls can be accurately estimated by the RC-TST/LER method, and the errors are within the same range as for reactions from the training set (R_2-R_{19}), thus proving the validity of the RC-TST/LER approximation.

3.4.3 Component error analysis

Finally, an analysis on the systematic errors in different factors in the RC-TST/LER methods was performed. These errors are from the use of fitted analytical expressions for the potential energy factor, tunneling factor, partition function factor, and hindered rotations factor introduced in the method. The deviations/errors between the approximated and exact factors within the TST framework are calculated at each temperature for every reaction in the representative set and then averaged over the whole class. For the LER approach, error in the potential energy factor comes from the use of the LER expression: that of the tunneling factor, from using three equations (Eqs. 10a, b); that of the partition function factor, from using Eqs. 11a, b; and that of the HR factor from using Eqs. 12a–c. It is important to note that mutual multiplication or cancelation of errors coming from different factors is possible. Absolute errors averaged over all 18 reactions, R_2–R_{19}, as functions of the temperature are plotted in Fig. 10. Of the factors, the HR and partition function ratios factor show the least temperature dependence for the whole temperature range. The tunneling factor introduces the smallest error of less than 10 % in the low temperature regime and almost equals to 0 for $T > 500$ K. The error from the partition function factor is largest for $T \approx 1{,}000$ K, and does not exceed 20 % for the whole temperature range. Error introduced by the AM1 LER potential energy factor decreases from 25 % at 300 K as the temperature increases. The error of the M062X LER potential energy factor is smaller than 40 %. Error introduced by the BGH potential energy factor is slightly larger, and AM1-based factor reaches 50 % at $T = 300$ K. Thus, the M062X LER approach gives less error in the potential energy factor than the BHG. The AM1 method yields the worst performance for this reaction class. For $T > 2{,}000$ K, the errors from both the LER and the BHG factors are almost the same; all of the errors are almost constant in this regime. For most cases, the total systematic errors due to the use of simple

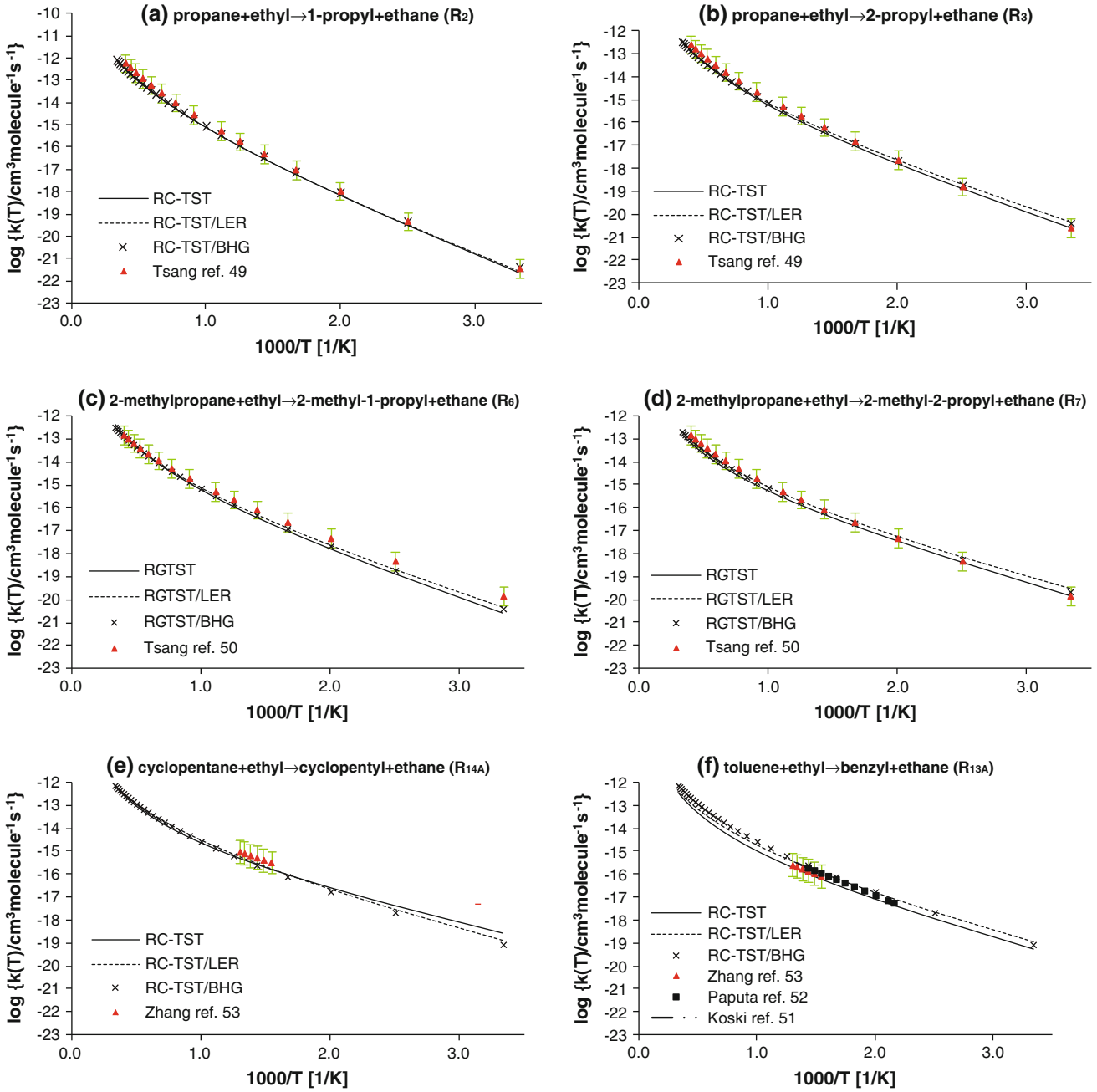

Fig. 7 Arrhenius plots of the calculated and experimental rate constants for the reactions: **a** propane + ethyl → 1-propyl + ethane (R_2) **b** propane + ethyl → 2-propyl + ethane (R_3) **c** 2-methylpropane + ethyl → 2-methyl-1-propyl + ethane (R_6) **d** 2-methylpropane + ethyl → 2-methyl-2-propyl + ethane (R_7) **e** toluene + ethyl → benzyl + ethane (R_{14A}) **f** cyclopentane + ethyl → cyclopentyl + ethane (R_{13A}). Experimental data are taken from: ref [49]. for reactions (**a**, **b**), ref [50]. for reactions (**c**, **d**), ref [51–53] for reaction (**e**), and ref [53] for reaction (**f**)

analytical expressions for different reaction class factors are less than 40 % for the temperature range 300–3,000 K. For the LER/AM1 approach, this error is larger but not to exceed 50 %. In general, if accurate rate constants needed, the M062X RC-TST/LER is recommended, while the BHG approach gives a quick estimation without doing any quantum chemistry calculation but with larger errors.

3.4.4 Comparison of potential energy factors obtained with different functionals

As mentioned in Sect. 2, it is of great interest to determine the sensitivity of RC-TST parameters with regard to the choice of DFT functional since previous applications of RC-TST method employed the BH&HLYP functional,

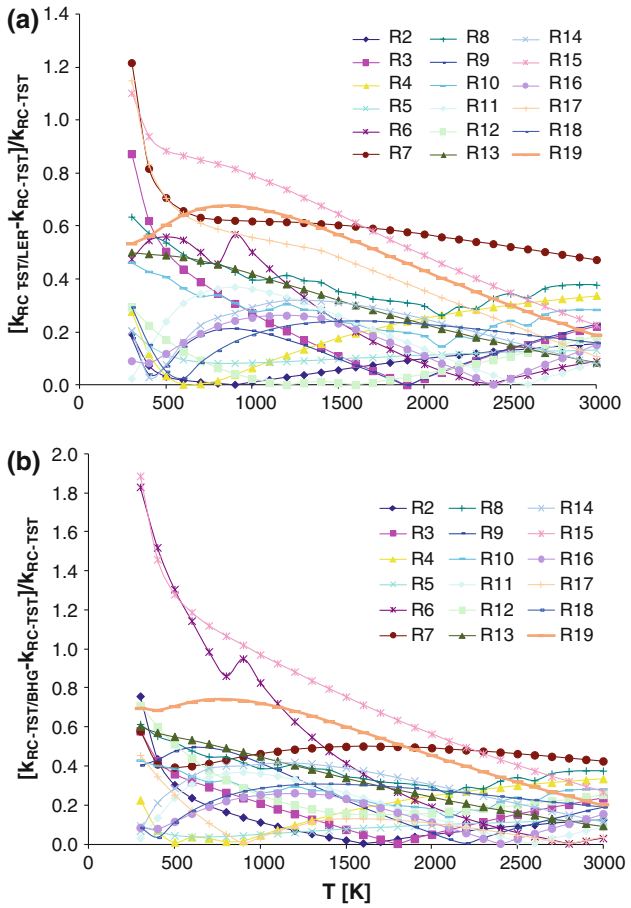

Fig. 8 **a**, **b** Relative absolute deviations as functions of the temperature between rate constants calculated from explicit TST/Eckart calculations for all selected reactions and: **a** from the RC-TST/LER method where M062X reaction energies were used for the LER **b** from the RCT-TST/BHG method

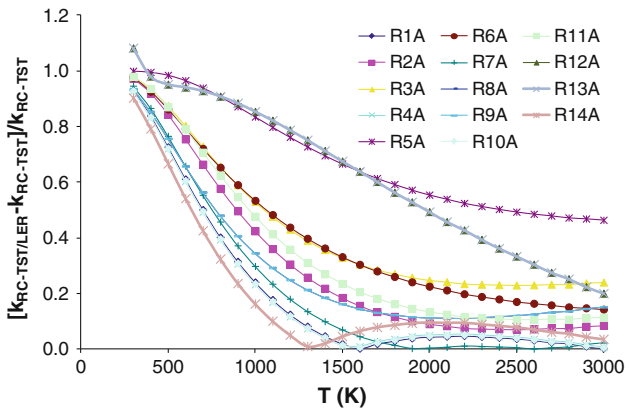

Fig. 9 Relative absolute deviations as functions of the temperature between rate constants calculated from explicit full RC-TST calculations for the reactions R_{1A}–R_{14A} and from the RC-TST/LER method, where M062X reaction energies were used for the LER

whereas in this study, we employed the M062X functional which is known to be more accurate for kinetics. Within the RC-TST framework, the potential energy factor is the most sensitive to the choice of the DFT functional and thus is used to address this issue here. Ratio of the potential energy factors calculated from M062X and BH&HLYP functionals is computed for each reaction and then averaged over all 19 reactions in the representative set. The result is plotted in Fig. 11. As one may expect, the ratio is more sensitive in the low temperature regime (see Eq. 6). Above 500 K, the difference in the potential energy factors from the two DFT functionals is less than 10 %. Below 500 K, the difference is larger but is still less than 20 % for the temperature range considered here. More importantly, the difference is smaller than the error range of the potential energy factors shown in Fig. 10. It is important to point out that even the difference in the absolute barrier heights calculated from both DFT functionals is about 2 kcal/mol, but the difference in the predicted rate constants using the RC-TST method is quite small. The key reason is that the RC-TST methodology uses only the relative barrier height, not absolute barrier height, and that

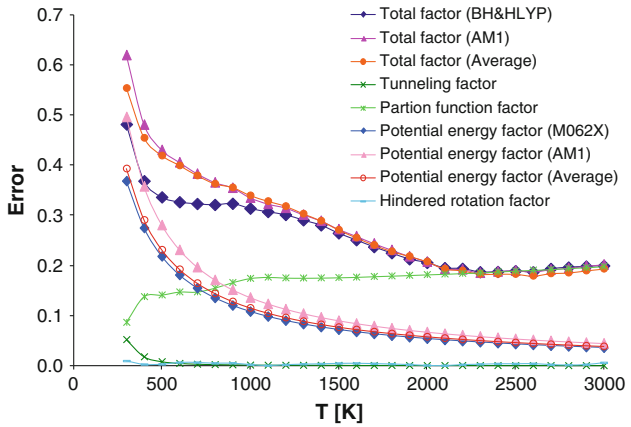

Fig. 10 Averaged absolute errors of the total relative rate factors $f(T)$ (Eq. 2) and its components, namely the partition function (f_Q), potential energy (f_V), and hindered rotation (f_{HR}) factors as functions of temperature

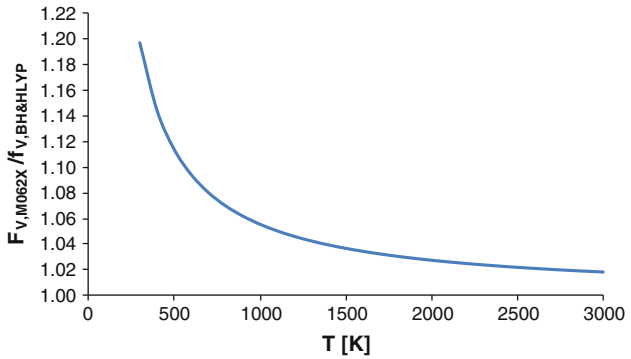

Fig. 11 Ratio of potential energy factors obtained with the M062X and BH&HLYP functionals

has proven to be less sensitive to the DFT functionals. This is the main advantage of the RC-TST methodology. Thus, one can conclude that the RC-TST results are not sensitive to the choice of the DFT functional.

3.5 Summary of approximations used in the RC-TST method

By generalizing from the small reference reaction to larger homologues and, consequently, enabling the obtaining of any rate constants within a given reaction class with accuracy comparable to high-level methods but at the fraction of the cost, the RS-TST method provides an effective way to derive considerable benefits from expensive electronic structure calculations. However, user should be aware of approximations used. In particular, these are as follows:

- Accuracy of RC-TST rate constants depends on the accuracy of the rate constants of the reference reaction.
- Although absolute transmission coefficients for hydrogen abstraction reactions often require multidimensional tunneling methods to account for the corner-cutting effects, it was shown [30] that, because of cancelation of errors, the tunneling factor f_κ can be accurately predicted using the 1-D Eckart method, as it is done in the RC-TST approach.
- The RC-TST method does not fully take into account the conformational aspects. For this reaction class, it assumed the effects of hindered rotation of different side chains are the same as of the methyl group. For larger alkyl groups, our previous study [29] showed that such approximation may yield error of about 10–20 % in the rate constants. Furthermore, it is not possible to exactly capture the changes of the numbers of free and hindered rotors for particular processes within the family; thus, the HR factor changes related to branching are only estimated, not exactly counted.
- The barrier height for any reaction within the family is calculated with the LER or BHG. Although, as shown in Table 1, error associated with these approximations is not large, it may affect the predicted rate constants particularly at low temperatures.

4 Conclusion

The application of the RC-TST combined with the LER (RC-TST/LER) and the BHG (RC-TST/BHG) approach to predict thermal rate constants for the reaction class of the hydrogen abstraction of alkanes by ethyl radical was carried out. The rate constants for the reference reaction $C_2H_6 + \cdot C_2H_5 \rightarrow \cdot C_2H_5 + C_2H_6$ were obtained by the CVT/SCT method in the temperature range of 300–3,000 K. All necessary parameters for predicting rate constants of any reaction in this class were derived from a training set of 19 representative reactions. The error analyses indicate that the RC-TST/LER method can predict rate constants within a factor of 2 as compared to explicit rate calculations. The performance for the RC-TST/BHG method is slightly worse. However, the convenience of ready to be used rate expressions for any reaction in the class would offset the less accuracy of the BHG approach as compared to that of the LER. Finally, it was found that RC-TST method is not sensitive to the choice of DFT functional used.

Acknowledgments The authors would like to thank the computational center of the University of Warsaw (ICM) for providing access to the supercomputer resources and the GAUSSIAN 09 program (Grant G33-03). An allocation of computer time at the Institute for Computational Science and Technology at Ho Chi Minh City is also gratefully acknowledged. This research was partially funded by Department of Science and Technology at Ho Chi Minh City and administrated by the Institute for Computational Science and Technology at Ho Chi Minh City.

References

1. Battin-Leclerc F (2008) Detailed chemical kinetic models for the low-temperature combustion of hydrocarbons with application to gasoline and diesel fuel surrogates. Prog Energ Combust Sci 34(4):440–498
2. Simmie J (2003) Detailed chemical kinetic models for the combustion of hydrocarbon fuels. Prog Energ Combust Sci 29(6): 599–634
3. Zádor J, Taatjes CA, Fernandes RX (2011) Kinetics of elementary reactions in low-temperature autoignition chemistry. Prog Energ Combust Sci 37(4):371–421
4. Guan Y, Yang B (2012) Kinetic modeling for hydrogen-abstraction reaction of methylcyclohexane with the CH_3 radical. Chem Eng Sci 79(1):200–209
5. Feng L-X, Jin L-X, Wang W-N, Wang W-L (2012) Mechanism and kinetics of the hydrogen abstraction reaction of C_2H_3 with CH_3F. Acta Phys Chim Sin 28(7):1623–1629
6. Kee RJ, Rupley FM, Miller JA (1995) Chemkin-II: a fortran chemical kinetics package for the analysis of gas-phase chemical kinetics:sandia report, SAND89-8009B
7. Marinov NM, Pitz WJ, Westbrook CK, Vincitore AM, Castaldi MJ, Senkan SM (1998) Aromatic and polycyclic aromatic hydrocarbon formation in a laminar premixed n-butane flame. Combust Flame 114(1–2):192–213
8. Curran HJ, Gaffuri P, Pitz WJ, Westbrook CK (1998) A comprehensive modeling study of n-heptane oxidation. Combust Flame 114(1–2):149–177
9. Curran HJ, Gaffuri P, Pitz WJ, Westbrook CK (2002) A comprehensive modeling study of iso-octane oxidation. Combust Flame 129(3):253–280

10. Truong TN (2000) Reaction class transition state theory: hydrogen abstraction reactions by hydrogen atoms as test cases. J Chem Phys 113(12):4957–4964
11. Sumathi R, Green WH (2002) A priori rate constants for kinetic modeling. Theor Chem Acc 108(4):187–213
12. Sumathi R, Carstensen HH, Green WH Jr (2001) Reaction rate prediction via group additivity part 1: H abstraction from alkanes by H and CH3. J Phys Chem A 105(28):6910–6925
13. Allen JW, Goldsmith CF, Green WH (2012) Automatic estimation of pressure-dependent rate coefficients. Phys Chem Chem Phys 14(3):1131–1155
14. Vandeputte AG, Sabbe MK, Reyniers M-F, Marin GB (2012) Kinetics of [small alpha] hydrogen abstractions from thiols, sulfides and thiocarbonyl compounds. Phys Chem Chem Phys 14(37):12773–12793
15. Sabbe MK, Reyniers MF, Waroquier M, Marin GB (2010) Hydrogen radical addition to unsaturated hydrocarbons and reverse beta-scission reactions: modeling of activation energies and pre-exponential factors. ChemPhysChem 11(1):195–210
16. Sabbe MK, Saeys M, Reyniers MF, Marin GB, Van Speybroeck V, Waroquier M (2007) Ab initio thermochemistry and kinetics for carbon-centered radical addition and β-scission reactions. J Phys Chem A 111(34):8416–8428
17. Sabbe MK, Vandeputte AG, Reyniers MF, Van Speybroeck V, Waroquier M, Marin GB (2007) Theoretical study of the thermodynamics and kinetics of hydrogen abstractions from hydrocarbons. J Phys Chem A 111(45):11771–11786
18. Wang HX, Wang BY, Zhang JL, Li ZR, Li XY (2011) Reaction class isodesmic reaction method and calculation of thermokinetic parameters for reactions in a class. Chem J Chin Univ 32(5):1123–1128
19. Wang B-Y, Tan N-X, Yao Q, Li Z-R, Li X-Y (2012) Accurate calculation of the reaction barriers and rate constants of the pyrolysis of alkyl radicals in the β position using the isodesmic reaction method. Acta Phys Chim Sin 28(12):2824–2830
20. Villano SM, Huynh LK, Carstensen H–H, Dean AM (2012) High-pressure rate rules for alkyl + O_2 reactions. 2. The isomerization, cyclic ether formation, and β-scission reactions of hydroperoxy alkyl radicals. J Phys Chem A 116(21):5068–5089
21. Villano SM, Huynh LK, Carstensen H–H, Dean AM (2011) High-pressure rate rules for alkyl + O2 reactions. 1. The dissociation, concerted elimination, and isomerization channels of the alkyl peroxy radical. J Phys Chem A 115(46):13425–13442
22. Carstensen H–H, Dean AM (2009) Rate constant rules for the automated generation of gas-phase reaction mechanisms. J Phys Chem A 113(2):367–380
23. Kungwan N, Truong TN (2005) Kinetics of the hydrogen abstraction ·CH3 + alkane = CH4 + alkyl reaction class: an application of the reaction class transition state theory. J Phys Chem A 109(34):7742–7750
24. Muszyńska M, Ratkiewicz A, Huynh LK, Truong TN (2009) Kinetics of the hydrogen abstraction $C_2H_3\cdot$ + alkane → C_2H_4 + alkyl radical reaction class. J Phys Chem A 113(29):8327–8336
25. Huynh LK, Truong TN (2007) Kinetics of the hydrogen abstraction CHO + alkane → HCHO + alkyl reaction class: an application of the reaction class transition state theory. Theor Chem Acc 120(1–3):107–118
26. Zhang S, Truong TN (2003) Kinetics of hydrogen abstraction reaction class H + H-C(sp3): first-principles predictions using the reaction class transition state theory. J Phys Chem A 107(8):1138–1147
27. Bankiewicz B, Huynh LK, Ratkiewicz A, Truong TN (2009) Kinetics of 1,4-hydrogen migration in the alkyl radical reaction class. J Phys Chem A 113(8):1564–1573
28. Ratkiewicz A, Bankiewicz B, Truong TN (2010) Kinetics of thermoneutral intramolecular hydrogen migration in alkyl radicals. Phys Chem Chem Phys 12(36):10988–10995
29. Ratkiewicz A, Truong TN (2012) Kinetics of the C–C bond beta scission reactions in alkyl radical reaction class. J Phys Chem A 116(25):6643–6654
30. Truong TN, Duncan WT, Tirtowidjojo M (1999) A reaction class approach for modeling gas phase reaction rates. Phys Chem Chem Phys 1(6):1061–1065
31. Daoutidis P, Marvin WA, Rangarajan S, Torres AI (2013) Engineering biomass conversion processes: a systems perspective. AIChE J 59(1):3–18
32. Frisch MJ, Trucks GW, Schlegel HB, Scuseria GE, Robb MA, Cheeseman JR, Scalmani G, Barone V, Mennucci B, Petersson GA, Nakatsuji H, Caricato M, Li X, Hratchian HP, Izmaylov AF, Bloino J, Zheng G, Sonnenberg JL, Hada M, Ehara M, Toyota K, Fukuda R, Hasegawa J, Ishida M, Nakajima T, Honda Y, Kitao O, Nakai H, Vreven T, Montgomery JA, Peralta JE, Ogliaro F, Bearpark M, Heyd JJ, Brothers E, Kudin KN, Staroverov VN, Kobayashi R, Normand J, Raghavachari K, Rendell A, Burant JC, Iyengar SS, Tomasi J, Cossi M, Rega N, Millam JM, Klene M, Knox JE, Cross JB, Bakken V, Adamo C, Jaramillo J, Gomperts R, Stratmann RE, Yazyev O, Austin AJ, Cammi R, Pomelli C, Ochterski JW, Martin RL, Morokuma K, Zakrzewski VG, Voth GA, Salvador P, Dannenberg JJ, Dapprich S, Daniels AD, Farkas, Foresman JB, Ortiz JV, Cioslowski J, Fox DJ (2009) Gaussian 09, Revision B01, Wallingford CT
33. Zhao Y, Truhlar D (2008) The M06 suite of density functionals for main group thermochemistry, thermochemical kinetics, noncovalent interactions, excited states, and transition elements: two new functionals and systematic testing of four M06-class functionals and 12 other functionals. Theor Chem Acc 120(1–3):215–241
34. Duncan WT, Bell RL, Truong TN (1998) TheRate: program for ab initio direct dynamics calculations of thermal and vibrational-state-selected rate constants. J Comp Chem 19(9):1039–1052
35. Ayala PY, Schlegel HB (1998) Identification and treatment of internal rotation in normal mode vibrational analysis. J Chem Phys 108(6):2314–2325
36. Dybala-Defratyka A, Paneth P, Pu J, Truhlar DG (1994) Benchmark results for hydrogen atom transfer between carbon centers and validation of electronic structure methods for bond energies and barrier heights. J Phys Chem A 108(13):2475–2486
37. Zheng J, Zhang S, Lynch BJ, Corchado JC, Chuang Y–Y, Fast PL, Hu W-P, Liu Y-P, Lynch GC, Nguyen KA, Jackels CF, Ramos AF, Ellingson BA, Melissas VS, Villà J, Rossi I, Coitiño EL, Pu J, Albu TV, Steckler R, Garret BC, Isaacson AD, Truhlar DG (2010) POLYRATE 2010-A: computer program for the calculation of chemical reaction rates for polyatomics. http://comp.chem.umn.edu/polyrate/
38. Fernández-Ramos A, Ellingson B, Meana-Pañeda R, Marques J, Truhlar D (2007) Symmetry numbers and chemical reaction rates. Theor Chem Acc 118(4):813–826
39. Davis AC, Tangprasertchai N, Francisco JS (2012) Hydrogen migrations in alkylcycloalkyl radicals: implications for chain-branching reactions in fuels. Chem Eur J 18(36):11296–11305
40. Comandini A, Awan IA, Manion JA (2012) Thermal decomposition of 1-pentyl radicals at high pressures and temperatures. Chem Phys Lett 552:20–26
41. Sirjean B, Dames E, Wang H, Tsang W (2012) Tunneling in hydrogen-transfer isomerization of n-alkyl radicals. J Phys Chem A 116(1):319–332
42. Awan IA, Burgess DR, Manion JA (2012) Pressure dependence and branching ratios in the decomposition of 1-pentyl radicals: shock tube experiments and master equation modeling. J Phys Chem A 116(11):2895–2910

43. Alecu IM, Truhlar DG (2011) Computational study of the reactions of methanol with the hydroperoxyl and methyl radicals. 1. Accurate thermochemistry and barrier heights. J Phys Chem A 115(13):2811–2829
44. Alecu IM, Truhlar DG (2011) Computational study of the reactions of methanol with the hydroperoxyl and methyl radicals. 2. Accurate thermal rate constants. J Phys Chem A 115(51):14599–14611
45. Cuccato D, Dossi M, Polino D, Cavallotti C, Moscatelli D (2012) Is quantum tunneling relevant in free-radical polymerization? Macromol React Eng 6(12):496–506
46. Engel PS, Gudimetla VB, Gancheff JS, Denis AP (2012) Solution phase photolysis of 1,2-dithiane alone and with single-walled carbon nanotubes. J Phys Chem A 116(32):8345–8351
47. Davis AC, Francisco JS (2011) Ab initio study of key branching reactions in biodiesel and fischer-troops fuels. J Am Chem Soc 133(47):19110–19124
48. Davis AC, Francisco JS (2011) Ab initio study of hydrogen migration across n-alkyl radicals. J Phys Chem A 115(14):2966–2977
49. Tsang W (1988) Chemical kinetic data base for combustion chemistry. Part 3: Propane. J Phys Chem Ref Data 17(2):887–951
50. Tsang W (1990) Chemical kinetic data base for combustion chemistry. Part 4: isobutane. J Phys Chem Ref Data 19(1):1–67
51. Koski AA, Price SJW, Trudell BC (1976) Studies of the pyrolysis of diethylzinc by the toluene carrier method and of the reaction of ethyl radicals with toluene. Can J Chem 54:482–487
52. Paputa MC, Price SJW (1979) Pyrolysis of triethylgallium by the toluene carrier technique. Can J Chem 57:3178–3181
53. Zhang HX, Ahonkhai SI, Back MH (1989) Rate constants for abstraction of hydrogen from benzene, toluene, and cyclopentane by methyl and ethyl radicals over the temperature range 650–770 K. Can J Chem 67:1541–1549